DESY 95-013
February 1995

Study of $D^*(2010)^{\pm}$ Production in ep Collisions at HERA

ZEUS Collaboration

February 7, 2008

arXiv:hep-ex/9502002v1 2 Feb 1995

Abstract

We report the first observation of charmed mesons with the ZEUS detector at HERA using the decay channel $D^{*+} \to (D^0 \to K^-\pi^+)\pi^+$ (+ c.c.). Clear signals in the mass difference $\Delta M{=}M(D^*){-}M(D^0)$ as well as in the $M(K\pi)$ distribution at the D^0 mass are found. The ep cross section for inclusive $D^{*\pm}$ production with $Q^2 < 4$ GeV^2 in the γp centre-of-mass energy range $115 < W < 275$ GeV has been determined to be $(32 \pm 7^{+4}_{-7})$ nb in the kinematic region $\{p_T(D^*) \geq 1.7$ GeV, $|\eta(D^*)| < 1.5\}$. Extrapolating outside this region, assuming a mass of the charm quark of 1.5 GeV, we estimate the ep charm cross section to be $\sigma(ep \to c\bar{c}X) = (0.45 \pm 0.11^{+0.37}_{-0.22})\,\mu$b at $\sqrt{s} = 296$ GeV and $\langle W \rangle = 198$ GeV. The average γp charm cross section $\sigma(\gamma p \to c\bar{c}X)$ is found to be $(6.3 \pm 2.2^{+6.3}_{-3.0})\,\mu$b at $\langle W \rangle = 163$ GeV and $(16.9 \pm 5.2^{+13.9}_{-8.5})\,\mu$b at $\langle W \rangle = 243$ GeV. The increase of the total charm photoproduction cross section by one order of magnitude with respect to low energy data experiments is well described by QCD NLO calculations using singular gluon distributions in the proton.

The ZEUS Collaboration

M. Derrick, D. Krakauer, S. Magill, D. Mikunas, B. Musgrave, J. Repond, R. Stanek, R.L. Talaga, H. Zhang
Argonne National Laboratory, Argonne, IL, USA [p]

R. Ayad[1], G. Bari, M. Basile, L. Bellagamba, D. Boscherini, A. Bruni, G. Bruni, P. Bruni, G. Cara Romeo, G. Castellini[2], M. Chiarini, L. Cifarelli[3], F. Cindolo, A. Contin, M. Corradi, I. Gialas, P. Giusti, G. Iacobucci, G. Laurenti, G. Levi, A. Margotti, T. Massam, R. Nania, C. Nemoz, F. Palmonari, A. Polini, G. Sartorelli, R. Timellini, Y. Zamora Garcia[1], A. Zichichi
University and INFN Bologna, Bologna, Italy [f]

A. Bargende, J. Crittenden, K. Desch, B. Diekmann[4], T. Doeker, M. Eckert, L. Feld, A. Frey, M. Geerts, G. Geitz[5], M. Grothe, T. Haas, H. Hartmann, D. Haun[4], K. Heinloth, E. Hilger, H.-P. Jakob, U.F. Katz, S.M. Mari, A. Mass, S. Mengel, J. Mollen, E. Paul, Ch. Rembser, R. Schattevoy[6], D. Schramm, J. Stamm, R. Wedemeyer
Physikalisches Institut der Universität Bonn, Bonn, Federal Republic of Germany [c]

S. Campbell-Robson, A. Cassidy, N. Dyce, B. Foster, S. George, R. Gilmore, G.P. Heath, H.F. Heath, T.J. Llewellyn, C.J.S. Morgado, D.J.P. Norman, J.A. O'Mara, R.J. Tapper, S.S. Wilson, R. Yoshida
H.H. Wills Physics Laboratory, University of Bristol, Bristol, U.K. [o]

R.R. Rau
Brookhaven National Laboratory, Upton, L.I., USA [p]

M. Arneodo[7], L. Iannotti, M. Schioppa, G. Susinno
Calabria University, Physics Dept.and INFN, Cosenza, Italy [f]

A. Bernstein, A. Caldwell, J.A. Parsons, S. Ritz, F. Sciulli, P.B. Straub, L. Wai, S. Yang, Q. Zhu
Columbia University, Nevis Labs., Irvington on Hudson, N.Y., USA [q]

P. Borzemski, J. Chwastowski, A. Eskreys, K. Piotrzkowski, M. Zachara, L. Zawiejski
Inst. of Nuclear Physics, Cracow, Poland [j]

L. Adamczyk, B. Bednarek, K. Eskreys, K. Jeleń, D. Kisielewska, T. Kowalski, E. Rulikowska-Zarębska, L. Suszycki, J. Zając
Faculty of Physics and Nuclear Techniques, Academy of Mining and Metallurgy, Cracow, Poland [j]

A. Kotański, M. Przybycień
Jagellonian Univ., Dept. of Physics, Cracow, Poland [k]

L.A.T. Bauerdick, U. Behrens, H. Beier[8], J.K. Bienlein, C. Coldewey, O. Deppe, K. Desler, G. Drews, M. Flasiński[9], D.J. Gilkinson, C. Glasman, P. Göttlicher, J. Große-Knetter, B. Gutjahr, W. Hain, D. Hasell, H. Heßling, H. Hultschig, Y. Iga, P. Joos, M. Kasemann, R. Klanner, W. Koch, L. Köpke[10], U. Kötz, H. Kowalski, J. Labs, A. Ladage, B. Löhr, M. Löwe, D. Lüke, O. Mańczak, J.S.T. Ng, S. Nickel, D. Notz, K. Ohrenberg, M. Roco, M. Rohde, J. Roldán, U. Schneekloth, W. Schulz, F. Selonke, E. Stiliaris[11], B. Surrow, T. Voß, D. Westphal, G. Wolf, C. Youngman, J.F. Zhou
Deutsches Elektronen-Synchrotron DESY, Hamburg, Federal Republic of Germany

H.J. Grabosch, A. Kharchilava, A. Leich, M. Mattingly, A. Meyer, S. Schlenstedt, N. Wulff
DESY-Zeuthen, Inst. für Hochenergiephysik, Zeuthen, Federal Republic of Germany

G. Barbagli, P. Pelfer
University and INFN, Florence, Italy [f]

G. Anzivino, G. Maccarrone, S. De Pasquale, L. Votano
INFN, Laboratori Nazionali di Frascati, Frascati, Italy [f]

A. Bamberger, S. Eisenhardt, A. Freidhof, S. Söldner-Rembold[12], J. Schroeder[13], T. Trefzger
Fakultät für Physik der Universität Freiburg i.Br., Freiburg i.Br., Federal Republic of Germany [c]

N.H. Brook, P.J. Bussey, A.T. Doyle[14], I. Fleck, D.H. Saxon, M.L. Utley, A.S. Wilson
Dept. of Physics and Astronomy, University of Glasgow, Glasgow, U.K. [o]

A. Dannemann, U. Holm, D. Horstmann, T. Neumann, R. Sinkus, K. Wick
Hamburg University, I. Institute of Exp. Physics, Hamburg, Federal Republic of Germany [c]

E. Badura[15], B.D. Burow[16], L. Hagge, E. Lohrmann, J. Mainusch, J. Milewski, M. Nakahata[17], N. Pavel, G. Poelz, W. Schott, F. Zetsche
Hamburg University, II. Institute of Exp. Physics, Hamburg, Federal Republic of Germany [c]

T.C. Bacon, I. Butterworth, E. Gallo, V.L. Harris, B.Y.H. Hung, K.R. Long, D.B. Miller, P.P.O. Morawitz, A. Prinias, J.K. Sedgbeer, A.F. Whitfield
Imperial College London, High Energy Nuclear Physics Group, London, U.K. [o]

U. Mallik, E. McCliment, M.Z. Wang, S.M. Wang, J.T. Wu, Y. Zhang
University of Iowa, Physics and Astronomy Dept., Iowa City, USA [p]

P. Cloth, D. Filges
Forschungszentrum Jülich, Institut für Kernphysik, Jülich, Federal Republic of Germany

S.H. An, S.M. Hong, S.W. Nam, S.K. Park, M.H. Suh, S.H. Yon
Korea University, Seoul, Korea [h]

R. Imlay, S. Kartik, H.-J. Kim, R.R. McNeil, W. Metcalf, V.K. Nadendla
Louisiana State University, Dept. of Physics and Astronomy, Baton Rouge, LA, USA [p]

F. Barreiro[18], G. Cases, R. Graciani, J.M. Hernández, L. Hervás[18], L. Labarga[18], J. del Peso, J. Puga, J. Terron, J.F. de Trocóniz
Univer. Autónoma Madrid, Depto de Física Teóríca, Madrid, Spain [n]

G.R. Smith
University of Manitoba, Dept. of Physics, Winnipeg, Manitoba, Canada [a]

F. Corriveau, D.S. Hanna, J. Hartmann, L.W. Hung, J.N. Lim, C.G. Matthews, P.M. Patel, L.E. Sinclair, D.G. Stairs, M. St.Laurent, R. Ullmann, G. Zacek
McGill University, Dept. of Physics, Montreal, Quebec, Canada [a, b]

V. Bashkirov, B.A. Dolgoshein, A. Stifutkin
Moscow Engineering Physics Institute, Mosocw, Russia [l]

G.L. Bashindzhagyan, P.F. Ermolov, L.K. Gladilin, Y.A. Golubkov, V.D. Kobrin, V.A. Kuzmin, A.S. Proskuryakov, A.A. Savin, L.M. Shcheglova, A.N. Solomin, N.P. Zotov
Moscow State University, Institute of Nuclear Pysics, Moscow, Russia [m]

M. Botje, F. Chlebana, A. Dake, J. Engelen, M. de Kamps, P. Kooijman, A. Kruse, H. Tiecke, W. Verkerke, M. Vreeswijk, L. Wiggers, E. de Wolf, R. van Woudenberg
NIKHEF and University of Amsterdam, Netherlands [i]

D. Acosta, B. Bylsma, L.S. Durkin, K. Honscheid, C. Li, T.Y. Ling, K.W. McLean[19], W.N. Murray, I.H. Park, T.A. Romanowski[20], R. Seidlein[21]
Ohio State University, Physics Department, Columbus, Ohio, USA [p]

D.S. Bailey, G.A. Blair[22], A. Byrne, R.J. Cashmore, A.M. Cooper-Sarkar, D. Daniels[23], R.C.E. Devenish, N. Harnew, M. Lancaster, P.E. Luffman[24], L. Lindemann, J.D. McFall, C. Nath, V.A. Noyes, A. Quadt, H. Uijterwaal, R. Walczak, F.F. Wilson, T. Yip
Department of Physics, University of Oxford, Oxford, U.K. [o]

G. Abbiendi, A. Bertolin, R. Brugnera, R. Carlin, F. Dal Corso, M. De Giorgi, U. Dosselli, S. Limentani, M. Morandin, M. Posocco, L. Stanco, R. Stroili, C. Voci
Dipartimento di Fisica dell' Universita and INFN, Padova, Italy [f]

J. Bulmahn, J.M. Butterworth, R.G. Feild, B.Y. Oh, J.J. Whitmore[25]
Pennsylvania State University, Dept. of Physics, University Park, PA, USA [q]

G. D'Agostini, G. Marini, A. Nigro, E. Tassi
Dipartimento di Fisica, Univ. 'La Sapienza' and INFN, Rome, Italy [f]

J.C. Hart, N.A. McCubbin, K. Prytz, T.P. Shah, T.L. Short
Rutherford Appleton Laboratory, Chilton, Didcot, Oxon, U.K. [o]

E. Barberis, N. Cartiglia, T. Dubbs, C. Heusch, M. Van Hook, B. Hubbard, W. Lockman, J.T. Rahn, H.F.-W. Sadrozinski, A. Seiden
University of California, Santa Cruz, CA, USA [p]

J. Biltzinger, R.J. Seifert, A.H. Walenta, G. Zech
Fachbereich Physik der Universität-Gesamthochschule Siegen, Federal Republic of Germany [c]

H. Abramowicz, G. Briskin, S. Dagan[26], A. Levy[27]
School of Physics,Tel-Aviv University, Tel Aviv, Israel [e]

T. Hasegawa, M. Hazumi, T. Ishii, M. Kuze, S. Mine, Y. Nagasawa, M. Nakao, I. Suzuki, K. Tokushuku, S. Yamada, Y. Yamazaki
Institute for Nuclear Study, University of Tokyo, Tokyo, Japan [g]

M. Chiba, R. Hamatsu, T. Hirose, K. Homma, S. Kitamura, Y. Nakamitsu, K. Yamauchi
Tokyo Metropolitan University, Dept. of Physics, Tokyo, Japan [g]

R. Cirio, M. Costa, M.I. Ferrero, L. Lamberti, S. Maselli, C. Peroni, R. Sacchi, A. Solano, A. Staiano
Universita di Torino, Dipartimento di Fisica Sperimentale and INFN, Torino, Italy [f]

M. Dardo
II Faculty of Sciences, Torino University and INFN - Alessandria, Italy [f]

D.C. Bailey, D. Bandyopadhyay, F. Benard, M. Brkic, M.B. Crombie, D.M. Gingrich[28], G.F. Hartner, K.K. Joo, G.M. Levman, J.F. Martin, R.S. Orr, C.R. Sampson, R.J. Teuscher
University of Toronto, Dept. of Physics, Toronto, Ont., Canada [a]

C.D. Catterall, T.W. Jones, P.B. Kaziewicz, J.B. Lane, R.L. Saunders, J. Shulman
University College London, Physics and Astronomy Dept., London, U.K. [o]

K. Blankenship, J. Kochocki, B. Lu, L.W. Mo
Virginia Polytechnic Inst. and State University, Physics Dept., Blacksburg, VA, USA [q]

W. Bogusz, K. Charchuła, J. Ciborowski, J. Gajewski, G. Grzelak, M. Kasprzak, M. Krzyżanowski, K. Muchorowski, R.J. Nowak, J.M. Pawlak, T. Tymieniecka, A.K. Wróblewski, J.A. Zakrzewski, A.F. Żarnecki
Warsaw University, Institute of Experimental Physics, Warsaw, Poland [j]

M. Adamus
Institute for Nuclear Studies, Warsaw, Poland [j]

Y. Eisenberg[26], U. Karshon[26], D. Revel[26], D. Zer-Zion
Weizmann Institute, Nuclear Physics Dept., Rehovot, Israel [d]

I. Ali, W.F. Badgett, B. Behrens, S. Dasu, C. Fordham, C. Foudas, A. Goussiou, R.J. Loveless, D.D. Reeder, S. Silverstein, W.H. Smith, A. Vaiciulis, M. Wodarczyk
University of Wisconsin, Dept. of Physics, Madison, WI, USA [p]

T. Tsurugai
Meiji Gakuin University, Faculty of General Education, Yokohama, Japan

S. Bhadra, M.L. Cardy, C.-P. Fagerstroem, W.R. Frisken, K.M. Furutani, M. Khakzad, W.B. Schmidke
York University, Dept. of Physics, North York, Ont., Canada [a]

[1] supported by Worldlab, Lausanne, Switzerland
[2] also at IROE Florence, Italy
[3] now at Univ. of Salerno and INFN Napoli, Italy
[4] now a self-employed consultant
[5] on leave of absence
[6] now at MPI Berlin
[7] now also at University of Torino
[8] presently at Columbia Univ., supported by DAAD/HSPII-AUFE
[9] now at Inst. of Computer Science, Jagellonian Univ., Cracow
[10] now at Univ. of Mainz
[11] supported by the European Community
[12] now with OPAL Collaboration, Faculty of Physics at Univ. of Freiburg
[13] now at SAS-Institut GmbH, Heidelberg
[14] also supported by DESY
[15] now at GSI Darmstadt
[16] also supported by NSERC
[17] now at Institute for Cosmic Ray Research, University of Tokyo
[18] on leave of absence at DESY, supported by DGICYT
[19] now at Carleton University, Ottawa, Canada
[20] now at Department of Energy, Washington
[21] now at HEP Div., Argonne National Lab., Argonne, IL, USA
[22] now at RHBNC, Univ. of London, England
[23] Fulbright Scholar 1993-1994
[24] now at Cambridge Consultants, Cambridge, U.K.
[25] on leave and partially supported by DESY 1993-95
[26] supported by a MINERVA Fellowship
[27] partially supported by DESY
[28] now at Centre for Subatomic Research, Univ.of Alberta, Canada and TRIUMF, Vancouver, Canada

[a] supported by the Natural Sciences and Engineering Research Council of Canada (NSERC)
[b] supported by the FCAR of Quebec, Canada
[c] supported by the German Federal Ministry for Research and Technology (BMFT)
[d] supported by the MINERVA Gesellschaft für Forschung GmbH, and by the Israel Academy of Science
[e] supported by the German Israeli Foundation, and by the Israel Academy of Science
[f] supported by the Italian National Institute for Nuclear Physics (INFN)
[g] supported by the Japanese Ministry of Education, Science and Culture (the Monbusho) and its grants for Scientific Research
[h] supported by the Korean Ministry of Education and Korea Science and Engineering Foundation
[i] supported by the Netherlands Foundation for Research on Matter (FOM)
[j] supported by the Polish State Committee for Scientific Research (grant No. SPB/P3/202/93) and the Foundation for Polish- German Collaboration (proj. No. 506/92)
[k] supported by the Polish State Committee for Scientific Research (grant No. PB 861/2/91 and No. 2 2372 9102, grant No. PB 2 2376 9102 and No. PB 2 0092 9101)
[l] partially supported by the German Federal Ministry for Research and Technology (BMFT)
[m] supported by the German Federal Ministry for Research and Technology (BMFT), the Volkswagen Foundation, and the Deutsche Forschungsgemeinschaft
[n] supported by the Spanish Ministry of Education and Science through funds provided by CICYT
[o] supported by the Particle Physics and Astronomy Research Council
[p] supported by the US Department of Energy
[q] supported by the US National Science Foundation

1 Introduction

In high energy ep collisions at HERA the leading order QCD contribution to charm production is the photon-gluon fusion (PGF) mechanism [1, 2]. In this process the photon participates as a point-like particle (*direct photon* process) interacting with a gluon from the proton and giving a $c\bar{c}$ pair ($\gamma g \to c\bar{c}$). The PGF cross section for $ep \to c\bar{c}X$ behaves like $d\sigma/dQ^2 \sim Q^{-2}$ and is dominated by the exchange of almost real photons ($Q^2 \approx 0$), i.e. by photoproduction events where the electron is scattered by a small angle. As a consequence, the contribution of the Deep Inelastic Scattering (DIS) regime, $Q^2 \gtrsim 4\,\mathrm{GeV}^2$, where the scattered electron is seen in the main detector, is expected to be small compared to photoproduction.

Apart from the *direct* channel, charm photoproduction at HERA can also proceed via the *resolved photon* processes [3, 4], where the photon behaves as a source of partons which can scatter off the partons in the proton (mainly $gg \to c\bar{c}$). QCD-based models predict that these types of processes dominate over the direct processes for light quark production [4, 5]. This prediction has been confirmed by measurements of the ZEUS [6, 7] and H1 [8] collaborations. The predicted open charm cross section at HERA has two major uncertainties: the mass of the charm quark (m_c) [9, 10] and the structure functions of the proton and the photon. Next to leading order (NLO) corrections have been calculated and found to be substantial [9, 11]. The full NLO cross section $\sigma(ep \to c\bar{c}X)$ at HERA, obtained using $m_c = 1.5$ GeV and the structure function parametrisation MRSD$'_-$ [12] for the proton and GRV HO [13] for the photon is predicted to be $\sim 0.9\,\mu$b [10] at $\sqrt{s} = 296$ GeV. A variation of m_c by ± 0.3 GeV changes the values of the cross sections by a factor of 2. The predicted relative amount of the direct and resolved contributions depends on the photon structure function parametrisation. For DG [14], GRV or ACFGP [15] the resolved contribution is less than 30%, but if the LAC1 [16] parametrisation is used the resolved contribution can be 50% or more and the predicted cross section can increase by almost a factor of 2. As a consequence, estimates of the total charm cross section $\sigma(ep \to c\bar{c}X)$ at HERA vary between 0.3 μb and 2 μb.

We search for open charm production at HERA with the ZEUS detector by looking for the fragmentation products of the heavy quarks which produce a $\mathrm{D}^*(2010)^{\pm}$. The method relies on the tight kinematic constraints of the decay chain[1]

$$\mathrm{D}^{*+} \to \mathrm{D}^0\pi_S^+ \to (\mathrm{K}^-\pi^+)\pi_S^+ \tag{1}$$

where the momentum of the pion coming from the D^* ('soft pion', π_S) is just 40 MeV in the D^* rest frame. Consequently, the mass difference [17]

$$\Delta M = M(\mathrm{D}^0\pi_S) - M(\mathrm{D}^0) = 145.42\,\mathrm{MeV}$$

can be measured much more accurately than the D^* mass itself. This low Q-value of the $\mathrm{D}^* \to \mathrm{D}^0\pi_S$ decay yields a prominent signal in an otherwise phase space suppressed kinematic region, the threshold of the $M(\mathrm{K}\pi\pi_S) - M(\mathrm{K}\pi)$ distribution.

We assume that the fraction of $\mathrm{D}^{*\pm}$ originating from $b\bar{b}$ is negligible [1].

[1] In this analysis the charge conjugated decay chain $\mathrm{D}^{*-} \to \bar{\mathrm{D}}^0\pi_S^- \to (\mathrm{K}^+\pi^-)\pi_S^-$ is also included.

2 Experimental Setup

Data were collected during the 1993 running period, when protons of energy $E_p = 820$ GeV were colliding with electrons of $E_e = 26.7$ GeV. Collisions took place between 84 electron and proton bunches with typical beam currents of 10 mA. Additional unpaired bunches of electrons and protons allowed an estimation of beam related background.

The total 1993 luminosity collected by ZEUS was ≈ 550 nb^{-1}, of which 486 nb^{-1} were used in the present work. This restricted sample contains runs taken with stable trigger conditions and the tracking chambers operating fully in the nominal magnetic field.

Charged particles are measured by the ZEUS inner tracking detectors, which operate in a magnetic field of 1.43 T provided by a thin superconducting coil. Immediately surrounding the beampipe is the vertex detector (VXD) [18] consisting of 120 radial cells, each with 12 sense wires. It uses a slow drift velocity gas and the presently achieved resolution is 50 μm in the central region of a cell and 150 μm near the edges. Surrounding the VXD is the central tracking detector (CTD) which consists of 72 cylindrical drift chamber layers, organised into 9 'superlayers' [19]. With our present calibration of the chamber, the resolution of the CTD is around 260 μm. The resolution in transverse momentum for tracks going through all superlayers is $\sigma(p_T)/p_T \approx \sqrt{(0.005)^2\, p_T^2 + (0.016)^2}$ where p_T is in GeV. The single hit efficiency is greater than 95%. The efficiency for assigning hits to tracks depends on several factors: very low p_T tracks suffer large systematic effects which reduce the probability of hits being attached to them, and the 45 degree inclination of the drift cells also introduces an asymmetry between positive and negative tracks. Nevertheless, the track reconstruction efficiency for tracks with $p_T > 0.1$ GeV is greater than 95%. Using the combined data from the VXD and CTD, resolutions of 0.4 cm in Z and 0.1 cm in radius in the XY plane[2] are obtained for the primary vertex reconstruction. From Gaussian fits to the Z vertex distribution, the r.m.s. spread is found to be 10.5 cm, in agreement with the expectation from the HERA proton bunch length.

The high resolution uranium-scintillator calorimeter (CAL) [20] is used in the present analysis to calculate global quantities of the events. It covers the polar angle range between $2.2^\circ < \theta < 176.5^\circ$, where $\theta = 0^\circ$ is the proton beam direction. It consists of three parts: the rear calorimeter (RCAL), covering the backward pseudorapidity[3] range $(-3.4 < \eta < -0.75)$; the barrel calorimeter (BCAL) covering the central region $(-0.75 < \eta < 1.1)$; and the forward calorimeter (FCAL) covering the forward region $(1.1 < \eta < 3.8)$. The calorimeter parts are subdivided into towers which in turn are subdivided longitudinally into electromagnetic (EMC) and hadronic (HAC) sections. The sections are subdivided into cells, each of which is viewed by two photomultiplier tubes. Under test beam conditions the CAL has an energy resolution, in units of GeV, of $\sigma_E = 0.35\sqrt{E(\mathrm{GeV})}$ for hadrons and $\sigma_E = 0.18\sqrt{E(\mathrm{GeV})}$ for electrons. The CAL also provides a time resolution of better than 1 ns for energy deposits greater than 4.5 GeV, and this timing is used for background rejection.

We use two lead-scintillator calorimeters (LUMI) [21] to measure the luminosity as well as to tag very small Q^2 processes. Bremsstrahlung photons emerging from the electron-proton interaction point (IP) at angles below 0.5 mrad with respect to the electron beam axis hit

[2]The ZEUS coordinate system is defined as right handed with the Z axis pointing in the proton beam direction, hereafter referred to as forward, and the X axis horizontal, pointing towards the centre of HERA.

[3]The pseudorapidity η is defined as $-\ln(\tan\frac{\theta}{2})$, where the polar angle θ is taken with respect to the proton beam direction.

the photon calorimeter 107 m from the IP. Electrons emitted from the IP at scattering angles $\pi - \theta'_e \leq 6$ mrad and with energies $0.2\ E_e < E'_e < 0.9\ E_e$ are deflected by beam magnets and hit the electron calorimeter placed 35 m from the IP.

3 Trigger Conditions

Data are collected with a three level trigger [22]. The hardwired First Level Trigger (FLT) is built as a deadtime free pipeline. The FLT decision is based on energy deposits in the calorimeter and luminosity detectors, on tracking information and on the muon chambers. We require a logical OR of five conditions on sums of energy in the calorimeter cells: either the BCAL EMC energy exceeds 3.4 GeV; or it exceeds 2.0 GeV, if any track is found in the CTD; or the RCAL EMC energy, excluding the towers immediately adjacent to the beam pipe, exceeds 2.0 GeV; or it exceeds 0.5 GeV, if any track is found in the CTD; or the RCAL EMC energy, including the beam pipe towers, exceeds 3.75 GeV.

The Second Level Trigger (SLT) uses information from a subset of detector components to separate physics events from backgrounds. It rejects proton beam-gas events using particle arrival times measured in the forward and rear sections of the calorimeter, reducing the FLT trigger rate by almost an order of magnitude.

The Third Level Trigger (TLT) has available most of the event information. It is used to apply stricter cuts on the event times and to reject beam-halo and cosmic muons. Beam-gas interactions are rejected by requiring:

- a reconstructed Z vertex position within 75 cm of the nominal interaction point,
- $\sum_i (E_i - p_{Zi}) > 3\,\mathrm{GeV}$,
- $\sum_i p_{Zi} / \sum_i E_i < 0.9$,

where the sums run over all calorimeter cells i and p_{Zi} is the Z-component of the momentum vector assigned to each cell of energy E_i.

The following additional TLT requirements are made in order to further reduce the background and the output rate:

- $(p_T^+)_{max} > 0.5$ GeV and $(p_T^-)_{max} > 0.5$ GeV and $(p_T^+)_{max} + (p_T^-)_{max} > 1.3$ GeV, where $(p_T^\pm)_{max}$ is the track of positive or negative charge with the highest p_T,
- transverse energy outside a cone of 10° around the proton direction in excess of 5 GeV; or $\sum_i (E_i - p_{Zi}) > 15\,\mathrm{GeV}$; or $\sum_i p_{Zi} / \sum_i E_i \leq 0.8$; or an electron with energy larger than 5 GeV detected in the LUMI electron calorimeter.

4 Kinematics

Neutral Current ep scattering $e\,(k)\,+\,p\,(P) \rightarrow e\,(k')\,+\,X$ can be described with the following kinematic variables:

$$\sqrt{s} = \sqrt{(k\,+\,P)^2} \approx \sqrt{4E_pE_e} = 296\,\mathrm{GeV}\,,$$

the total ep centre of mass energy;

$$q^2 = -Q^2 = (k\,-\,k')^2\,,$$

the four-momentum transfer squared carried by the virtual photon;

$$y = \frac{q \cdot P}{k \cdot P}\,,$$

the Bjorken variable describing the energy transfer to the hadronic system; and

$$W^2 = (q+P)^2 = -Q^2 + ys + m_p^2\,,$$

the centre of mass energy squared of the γp system, where m_p is the mass of the proton.

The variable y can be determined to a good approximation from the hadronic system using the Jacquet-Blondel expression [23]:

$$y_{JB} = \frac{\sum_i (E_i - p_{Zi})}{2 \cdot E_e}$$

with the sum running over all calorimeter cells i except for those associated with the scattered electron.

If the scattered electron is seen in the main detector (DIS events) or in the LUMI electron calorimeter (tagged photoproduction events), the variable y can also be obtained from:

$$y_e = 1 - \frac{E'_e}{E_e}\,\frac{1 - cos\theta'_e}{2}.$$

5 Monte Carlo Simulation

The Monte Carlo programs HERWIG[24] and PYTHIA[25] are used to model the hadronic final states in $c\bar{c}$ production. Both generators include parton showers in the initial and final states. Fragmentation into hadrons is simulated with the LUND string model [26] as implemented in JETSET[27] in the case of PYTHIA, and with a cluster algorithm in the case of HERWIG. The lepton-photon vertex is modelled according to the Weizsäcker-Williams Approximation (WWA) [28] in the case of PYTHIA, whereas HERWIG uses exact matrix elements for the photon-gluon fusion (PGF) component and the Equivalent Photon Approximation (EPA) [29] for resolved processes.

For these Monte Carlo models a large number of $c\bar{c}$ events was generated, but only those containing at least one charged D^*, decaying into $D^0\pi_S$ with subsequent decay $D^0 \rightarrow K\pi$, were

processed through the standard ZEUS detector and trigger simulation programs and through the event reconstruction package. With both Monte Carlo programs we have generated events with both direct and resolved components, setting $m_c = 1.5\,\mathrm{GeV}$. The parton densities in the proton were described by MRSD′_ and by GRV HO in the case of the photon. For systematic checks, we also generated events using different parametrisations for the proton (MRSD$'_0$ [12], CTEQ2M′ [30] and GRV HO [31]) and the photon (DG, ACFGP and LAC1). To check the dependence of the results on the charm mass assumed in the Monte Carlo simulations the whole analysis was repeated using the default values for m_c in both Monte Carlo generators (1.35 GeV in PYTHIA and 1.8 GeV in HERWIG).

6 D* Observation

6.1 Reconstruction Method

In order to select a kinematic region where the efficiency of the tracking detectors is high and systematic uncertainties are well understood, the following requirements on the tracks are made:

- $p_T > 0.16\,\mathrm{GeV}$;
- $|\eta| < 1.5$, corresponding to $25^\circ < \theta < 155^\circ$.

Pairs of these tracks with opposite charge are combined and considered in turn to be a kaon or a pion. The combination is accepted as a possible D^0 candidate if the Kπ invariant mass lies in the range:

$$1.80 < M(K\pi) < 1.93\,\mathrm{GeV}$$

(the nominal value of the D^0 mass is 1.865 GeV [17]). To reconstruct D^* mesons, these D^0 candidates are combined with an additional track having opposite charge to that of the kaon. Assuming this third track to be the soft pion, the mass difference $\Delta M = M(\mathrm{K}\pi\pi_S) - M(\mathrm{K}\pi)$ is then evaluated.

Monte Carlo studies show that after these cuts more than 95% of the decay products of the D^0 satisfy $p_T > 0.5$ GeV, with a mean value of 1.5 GeV. These high transverse momentum tracks have a higher reconstruction efficiency and a better track extrapolation to the vertex. As a consequence, the following more stringent cut is applied to them:

$$p_T(K), p_T(\pi) > 0.5\,\mathrm{GeV}.$$

From Monte Carlo studies we find that the π_S travels essentially in the same direction as the D^* itself. Therefore the $|\eta| < 1.5$ cut on the single tracks limits the $\eta(\mathrm{D}^*)$ range to:

$$|\eta(\mathrm{D}^*)| < 1.5.$$

This cut was thus also applied.

Moreover, we have restricted our analysis to:

$$p_T(\mathrm{D}^*) > 1.7\,\mathrm{GeV},$$

since more than 95% of the D^*'s fulfil this condition after the above cuts.

6.2 ΔM and $M(\mathrm{D}^0)$ Signals

DIS events are defined to be those having an electron identified in the CAL with $y_e < 0.7$. The Q^2 for these events is larger than 4 GeV^2. We find that 20% of the events in which we find a D* candidate fulfil this requirement. This relatively large fraction of DIS candidates, reproduced by the Monte Carlo programs, is due to the higher trigger acceptance for DIS events than for photoproduction events, and to the harder $p_T(\mathrm{D}^*)$ and $p_T(\pi_S)$ spectrum for these events. We show the ΔM distribution for the DIS candidates in Fig. 1. A clear $\mathrm{D}^{*\pm}$ signal around the nominal value of ΔM is observed which is evidence for $\mathrm{D}^{*\pm}$ production at HERA in DIS with $Q^2 > 4\,\mathrm{GeV}^2$.

The 80% of the D* candidates which are not identified as DIS events have $Q^2 < 4\,\mathrm{GeV}^2$ and are called photoproduction events. Of these, 27% are tagged in the LUMI electron calorimeter, in agreement with Monte Carlo simulations and the ZEUS photoproduction measurements [6]. To reduce possible background from DIS, where the electron is not identified, we require $y_{JB} < 0.7$ [7]. The true W and y are underestimated using the Jacquet-Blondel method. We correct the measured W_{JB} with Monte Carlo methods [32], resulting in a corrected W value which will be used in the following. Comparison with the W measured from events with a LUMI tag shows that the estimated true W has a systematic uncertainty of less than 10%. The cut on y_{JB} corresponds to $W < 275$ GeV. Furthermore we will restrict ourselves to $W > 115$ GeV where the acceptance is above 8%. The ΔM distribution for these photoproduction events obtained with the set of cuts described above is shown in Fig. 2a. A clear peak around $\Delta M = 145.5$ MeV is observed.

In order to check the background shape, pairs of tracks with the same charge are selected for calculating the $K\pi$ invariant mass (wrong charge combination method). This distribution is fitted with the maximum-likelihood method using the function: $A \times (\Delta M - m_\pi)^B$, where A and B are the free parameters of the fit.

The signal distribution is then fitted assuming this function for the background plus a Gaussian to parametrise the signal shape. The corresponding fits and the normalised background are also shown in Fig. 2a. The background shape parameters obtained in the signal fit agree with the values obtained by fitting the wrong charge distribution.

We observe 48 ± 11 D*'s above background, with a signal to background ratio of about 1.5. The mean value of the ΔM signal obtained from the fit is $\Delta M = (145.4 \pm 0.2)$ MeV, consistent with the nominal value. The corresponding width is (0.9 ± 0.2) MeV, in agreement with 0.7 MeV obtained from Monte Carlo simulation. The mean W for these events is $\langle W \rangle = 198$ GeV.

To check whether the D*'s are produced according to the decay channel (1), we show in Fig. 2b the $M(\mathrm{K}\pi)$ distribution for the events in the ΔM range from 142 MeV to 149 MeV. A clear signal is seen around the nominal value of the D^0 mass. In order to fit this distribution we have used an exponential background shape plus a Gaussian for the signal. The number of observed D^0's is 43 ± 12, consistent with the number of D*'s obtained from the fit to the ΔM distribution. We obtain a mean value of $M(\mathrm{D}^0) = (1.854 \pm 0.005)$ GeV, slightly below the nominal value, with a width of (18 ± 4) MeV, consistent with the value of 17 MeV obtained from Monte Carlo simulation.

7 Cross Sections

7.1 *ep* Cross Section

The cross section is obtained using the expression:

$$\sigma = \frac{N}{\mathcal{L} \times BR \times Acc},$$

where $N = 48$ is the number of observed D*'s, $\mathcal{L} = 486$ nb^{-1} is the integrated luminosity, and $BR = (2.73 \pm 0.11)\%$ [17] is the combined branching ratio of the decay chain (1). The acceptance Acc was calculated as the number of detected over generated $\mathrm{D}^* \to \mathrm{K}\pi\pi_S$ decays in the kinematic range chosen, using Monte Carlo methods including the trigger simulation. We have used the PYTHIA Monte Carlo prediction with MRSD'_/GRV HO structure function parametrisations for the proton/photon to correct our data and quote cross sections. The overall acceptance in the kinematic region $\{p_T(\mathrm{D}^*) > 1.7$ GeV, $|\eta(\mathrm{D}^*)| < 1.5\}$ for the W range from 115 to 275 GeV is $Acc = 11.4\%$ for the above Monte Carlo program.

We describe here the checks that are found to have a significant contribution to the systematic error. For the acceptance, a systematic shift of +18% is estimated using different structure function parametrisations and +14% using HERWIG with MRSD'_/GRV HO as a different Monte Carlo program. Also, a systematic error of 8% is found by varying the cuts on $p_T(K, \pi)$ between 0.3 GeV and 0.7 GeV and on $p_T(\pi_S)$ between 0.1 GeV and 0.25 GeV. Adding these errors in quadrature yields a total systematic error in the acceptance calculation of $^{+24}_{-8}\%$. The systematic error on the number of events is 10%, estimated by using different background parametrisations to fit the signals. The systematic error of the luminosity measurement is 3.3%.

Using the above quantities we measure an *ep* cross section for $\mathrm{D}^{*\pm}$ production, $\sigma(ep \to \mathrm{D}^{*\pm}X) \equiv \sigma(ep \to \mathrm{D}^{*+}X) + \sigma(ep \to \mathrm{D}^{*-}X)$, of:

$$\sigma(ep \to \mathrm{D}^{*\pm}X) = 32 \pm 7(stat)^{+4}_{-7}(syst) \text{ nb}$$

in the kinematic region $\{p_T(\mathrm{D}^*) > 1.7$ GeV, $|\eta(\mathrm{D}^*)| < 1.5\}$ and $115 < W < 275$ GeV. This cross section is valid for $Q^2 < 4$ GeV^2. The statistical error also includes the one due to the Monte Carlo statistics.

In order to quote a cross section for charm production we need to correct for the fraction of events in which a charm quark pair fragments into D^{*+} or D^{*-} as well as for the acceptance A_{ext} of the kinematic region $\{p_T(\mathrm{D}^*) > 1.7$ GeV, $|\eta(\mathrm{D}^*)| < 1.5\}$. The former is $(52.0 \pm 4.2)\%$ [33] and the latter is calculated by using PYTHIA with MRSD'_/GRV HO to be $A_{ext} = 13.7\%$ for the region $115 < W < 275$ GeV. This extrapolation outside the kinematic region has a large uncertainty. In extrapolating $p_T(\mathrm{D}^*)$, the uncertainty is mainly due to the strong dependence on the m_c value and for $\eta(\mathrm{D}^*)$ it comes from the large differences between the different structure function parametrisations in the region $|\eta(\mathrm{D}^*)| > 1.5$. As a consequence, the systematic error of the product $Acc \cdot A_{ext}$ is very large. We have fixed m_c to 1.5 GeV and quote the systematic error $\Delta(Acc \cdot A_{ext})$ coming from the different structure functions and using HERWIG (SF and MC in Table 1 respectively). Using a value of m_c of 1.35 GeV (1.8 GeV) results in a shift of +25% (−40%) of the estimated cross section.

$\langle W \rangle$ (GeV)	N	Acc (%)	A_{ext} (%)	$\Delta(Acc \cdot A_{ext})$ SF	MC	$\sigma(ep \to c\bar{c}X)$ (μb)	Integrated Φ	$\sigma(\gamma p \to c\bar{c}X)$ (μb)
163 ± 16	21 ± 7	8.1	16.2	$^{+63}_{-49}\%$	+54%	$0.23 \pm 0.08^{+0.23}_{-0.11}$	0.0367	$6.3 \pm 2.2^{+6.3}_{-3.0}$
243 ± 24	28 ± 8	22.4	8.8	$^{+92}_{-43}\%$	+30%	$0.21 \pm 0.06^{+0.17}_{-0.10}$	0.0122	$16.9 \pm 5.2^{+13.9}_{-8.5}$
198 ± 20	48 ± 11	11.4	13.7	$^{+76}_{-43}\%$	+48%	$0.45 \pm 0.11^{+0.37}_{-0.22}$	0.0488	$9.1 \pm 2.2^{+7.6}_{-4.4}$

Table 1: Acceptances and cross sections

We therefore estimate the ep charm production cross section at $\sqrt{s} = 296$ GeV for $Q^2 < 4$ GeV^2 in the range $115 < W < 275$ GeV as:

$$\sigma(ep \to c\bar{c}X) = 0.45 \pm 0.11^{+0.37}_{-0.22}\ \mu\text{b}.$$

This procedure was also carried out dividing W into two ranges, $115 < W < 205$ GeV and $205 < W < 275$ GeV. The $\langle W \rangle$ for the events in these two ranges were 163 GeV and 243 GeV respectively. The error in W is dominated by the systematic uncertainty of the Jacquet-Blondel method. The results are shown in Table 1.

7.2 γp Cross Section

The γp cross section can be obtained from the corresponding ep cross section using the EPA formula:

$$\sigma_{ep}(s) = \int_{y_{min}}^{y_{max}} dy \int_{Q^2_{min}}^{Q^2_{max}} dQ^2 \cdot \Phi(y, Q^2) \cdot \sigma_{\gamma^* p}(W, Q^2),$$

where

$$\Phi(y, Q^2) = \frac{\alpha}{2\pi} \frac{1}{yQ^2} [1 + (1-y)^2 - \frac{2m_e^2 y^2}{Q^2}]$$

is the flux of transverse photons, $Q^2_{min} = m_e^2 \frac{y^2}{1-y}$, $Q^2_{max} = 4\,\text{GeV}^2$ and m_e is the electron mass. Since the median $Q^2 \approx 10^{-4}$ GeV^2 is very small, we can assume the photons to be on-shell and therefore neglect the longitudinal contribution and the Q^2 dependence of $\sigma_{\gamma p}$. The γp cross section is then obtained as the ratio of the measured ep cross section and the photon flux factor Φ integrated over the Q^2 and y range covered by the measurement. This procedure assumes that $\sigma_{\gamma p}(W)$ is independent of y in the range of the measurement. As this dependence is not known a priori, the above calculation procedure was repeated assuming a proportional or logarithmic rise in W. An increase of 5% in the resulting cross section was found at $\langle W \rangle = 163$ GeV and less than 2% at $\langle W \rangle = 243$ GeV.

The estimated charm photoproduction cross section is $(6.3 \pm 2.2^{+6.3}_{-3.0})\,\mu$b at $\langle W \rangle = 163$ GeV and $(16.9 \pm 5.2^{+13.9}_{-8.5})\,\mu$b at $\langle W \rangle = 243$ GeV, assuming $m_c = 1.5$ GeV (see Table 1). In Fig. 3 we show our measurements for the total $c\bar{c}$ photoproduction cross section as a function of W, in addition to earlier measurements in fixed target experiments [35] and NLO QCD calculations [34] for $m_c = 1.5$ GeV. The solid line represents the prediction with the MRSD'_/GRV HO structure function parametrisation for proton/photon using $\mu_R = m_c$ as the renormalisation scale. The shaded band represents the theoretical uncertainties coming from varying this scale in the

range $0.5 < \mu_R/m_c < 2$. We also show the extreme predictions of MRSD′_/LAC1 (dashed line) and MRSD′$_0$/GRV HO (dash-dotted line) for $\mu_R = m_c$. We note that our measurement of the total charm photoproduction cross section at these high W values is in good agreement with those calculated using singular gluon distributions in the proton like MRSD′_ or GRV [36].

8 Summary

We have observed 48 $\mathrm{D}^*(2010)^{\pm}$ mesons in the decay channel $\mathrm{D}^{*+} \to \mathrm{D}^0\pi^+ \to (\mathrm{K}^-\pi^+)\pi^+$ (+ c.c.) in photoproduction events from ep collisions at HERA. Cross sections have been determined for these events with $Q^2 < 4\,\mathrm{GeV}^2$ and $115 < W < 275$ GeV. The ep cross section for inclusive $\mathrm{D}^{*\pm}$ production is found to be $(32 \pm 7^{+4}_{-7})$ nb in the kinematic region $\{p_T(\mathrm{D}^*) > 1.7$ GeV, $|\eta(\mathrm{D}^*)| < 1.5\}$. Extrapolating outside this region and assuming a mass of the charm quark of 1.5 GeV we estimate the ep charm cross sections to be $\sigma(ep \to c\bar{c}X) = (0.45 \pm 0.11^{+0.37}_{-0.22})\,\mu$b at $\sqrt{s} = 296$ GeV and $115 < W < 275$ GeV. The average γp charm cross section $\sigma(\gamma p \to c\bar{c}X)$ is found to be $(6.3 \pm 2.2^{+6.3}_{-3.0})\,\mu$b at $\langle W \rangle = 163$ GeV and $(16.9 \pm 5.2^{+13.9}_{-8.5})\,\mu$b at $\langle W \rangle = 243$ GeV. NLO QCD calculations using a gluon momentum density in the proton $\sim x^{-1/2}$ at low x are in good agreement with the observed increase of the cross section by one order of magnitude when the γp centre-of-mass energy increases one order of magnitude with respect to previous low energy experiments.

Acknowledgements

We thank the DESY Directorate for their strong support and encouragement. The remarkable achievements of the HERA machine group were essential for the successful completion of this work, and are gratefully appreciated. We also gratefully acknowledge the support of the DESY computing and network services. We thank S. Frixione, M.L. Mangano, P. Nason, and G. Ridolfi, for providing us with their results for the curves in Fig. 3.

References

[1] A. Ali et al., in Proc. of the HERA Workshop, DESY (1987) 395.

[2] R. van Woudenberg et al., in Proc. of the Workshop *Physics at HERA*, DESY (1991) 739.

[3] E. Witten, Nucl. Phys. B120 (1977) 189;
J.F. Owens, Phys. Rev. D21 (1980) 54.

[4] M. Drees and F. Halzen, Phys. Rev. Lett. 61 (1988) 275;
G.A. Schuler and T. Sjöstrand, Phys. Lett. B300 (1993) 169.

[5] L.E. Gordon and J.K. Storrow, Phys. Lett. B291 (1992) 320;
D. Bödeker, Phys. Lett. B292 (1992) 164.

[6] ZEUS Collab., M. Derrick et al., Phys. Lett. B297 (1992) 404.

[7] ZEUS Collab., M. Derrick et al., Phys. Lett. B322 (1994) 287.

[8] H1 Collab., T.Ahmed et al., Phys. Lett. B297 (1992) 205.

[9] R.K. Ellis and P. Nason, Nucl. Phys. B312 (1989) 551.

[10] S. Frixione et al., Phys. Lett. B308 (1993) 137.

[11] P. Nason, S. Dawson and R.K. Ellis, Nucl. Phys. B303 (1988) 607;
J. Smith and W.L. van Neerven, Nucl. Phys. B374 (1992) 36.

[12] A.D. Martin, W.J. Stirling and R.G. Roberts, Phys. Lett. B306 (1993) 145.

[13] M. Glück, E. Reya and A. Vogt, Phys. Lett. B306 (1993) 391.

[14] M. Drees and K. Grassie, Z. Phys. C28 (1985) 451.

[15] P. Aurenche et al., Z. Phys. C56 (1992) 589.

[16] H. Abramowicz, K. Charchuła and A. Levy, Phys. Lett. B269 (1991) 458.

[17] Particle Data Group, Review of Particle Properties, Phys. Rev. D50, (1994) 1173.

[18] C. Alvisi et al., Nucl. Instr. Meth. A305 (1991) 30.

[19] N. Harnew et al., Nucl. Instr. Meth. A279 (1989) 290;
B. Foster et al., Nucl. Phys. B (Proc. Suppl.) 32 (1993) 181 and Nucl. Inst. Meth. A338 (1994) 254.

[20] A. Andresen et al. Nucl. Inst. Meth. A309 (1991) 101;
A. Caldwell et al., Nucl. Inst. Meth. A321 (1992) 352.
A. Bernstein et al., Nucl. Inst. Meth. A336 (1993) 23;

[21] J. Andruszków et al., DESY preprint, DESY 92–066 (1992).

[22] The ZEUS Detector, Status Report 1993, DESY 1993;
W.H. Smith et al., DESY preprint, DESY 94–183 (1994).

[23] F. Jacquet and A. Blondel, Proc. of the Study for an *ep* Facility for Europe, ed. U. Amaldi, DESY 79/48 (1979) 391.

[24] G. Marchesini et al., Comp. Phys. Comm. 67 (1992) 465.

[25] T. Sjöstrand, Z. Phys. C42 (1989) 301 and in Proc. of the Workshop *Physics at HERA*, DESY (1991) 1405.

[26] B. Andersson et al., Phys. Rep. 97 (1983) 31.

[27] T. Sjöstrand, Comp. Phys. Comm. 39 (1986) 347;
T. Sjöstrand and M. Bengtsson, Comp. Phys. Comm. 43 (1987) 367.

[28] C.F. Weizsäcker, Z.Phys. 88 (1934) 612;
E.J.Williams, Phys.Rev. 45 (1934) 729.

[29] V.M. Budnev et al., Phys. Rep. C15 (1975) 181.

[30] W.K. Tung, Proccedings of International Workshop on Deep Inelastic Scattering and Related Subjects, Eilat, Israel, 1994 World Sci., Singapore, to be published;
H.L. Lai et al., MSU-HEP-41024, Oct. 1994, to be published.

[31] M.Glück, E.Reya and A.Vogt, Z. Phys. C53 (1992) 127.

[32] ZEUS Collab., M. Derrick et al., DESY preprint, DESY-94-176.

[33] OPAL Collab., G. Alexander et al., Phys. Lett. B262 (1991) 341, updated in ICHEP94 Ref. 0513, to be published in Z. Phys. C.

[34] S. Frixione, M.L. Mangano, P. Nason and G. Ridolfi, private communication. See also Nucl. Phys. B412 (1994) 225 and CERN-TH.7292/94, GEF-TH-4/1994, to be published in Nucl. Phys. B.

[35] CIF Collab., M.S. Atiya et al., Phys. Rev. Lett. 43 (1979) 414;
BFP Collab., A.R. Clark et al., Phys. Rev. Lett. 45 (1980) 682;
SLAC HFP Collab., K. Abe et al., Phys. Rev. D30 (1984) 1;
EMC Collab., M. Arneodo et al., Z. Phys. C35 (1987) 1;
PEC Collab., M. Adamovich et al., Phys. Lett. B187 (1987) 437;
E691 Collab., J.C. Anjos et al., Phys. Rev. Lett. 65 (1990) 2503;
NA-14′ Collab., M.P. Alvarez et al., Z. Phys. C60 (1993) 53.

[36] M. Glück, E. Reya and A. Vogt, Phys. Lett. B285 (1992) 285.

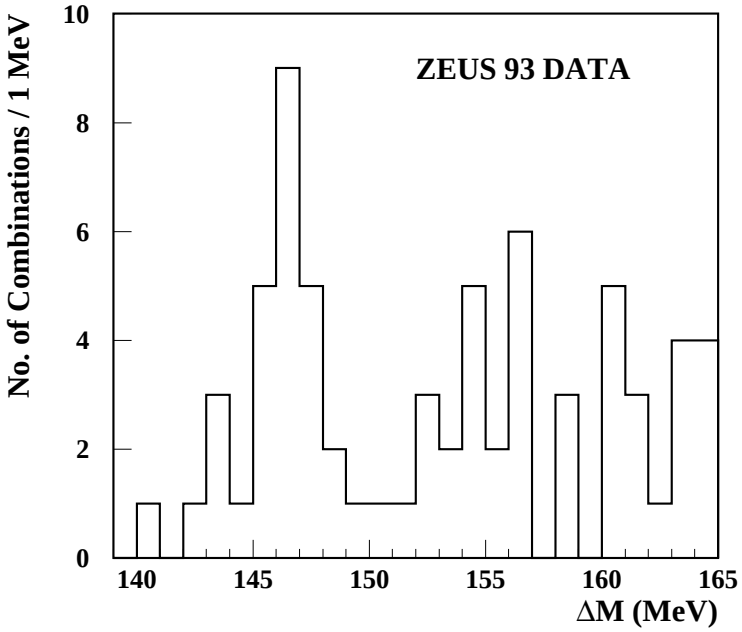

Figure 1: $\Delta M = M(\mathrm{K}\pi\pi_S) - M(\mathrm{K}\pi)$ distribution for DIS candidates : $Q^2 \geq 4\,\mathrm{GeV}^2$ and $y_e < 0.7$.

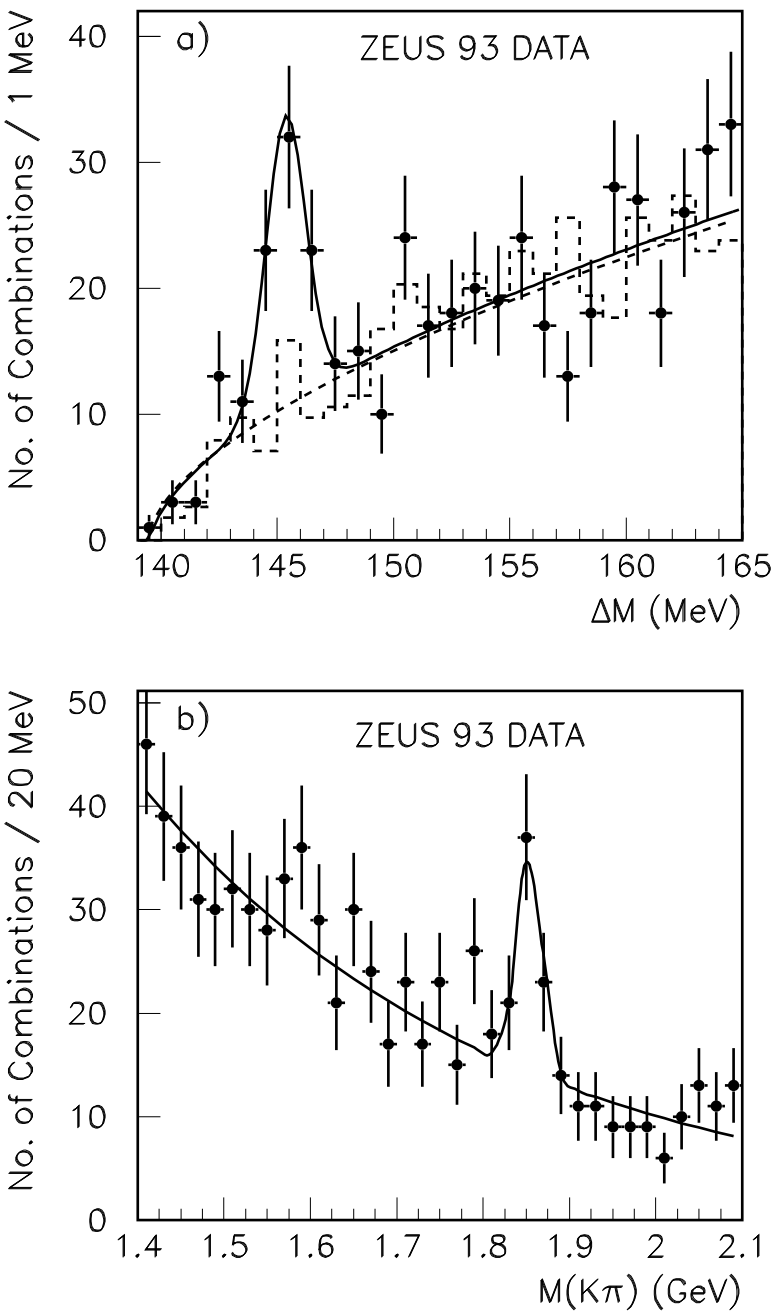

Figure 2: a) ΔM distribution for photoproduction events having $1.80 < M(K\pi) < 1.93$ GeV: signal (dots) and wrong charge combinations (dashed histogram). The dashed line is a fit to the wrong charge background using the parametrisation $A(\Delta M - m_\pi)^B$, where m_π is the mass of the pion. The solid line is a fit to the distribution, parametrised as a sum of the same function for the background plus a Gaussian for the signal. b) $(K\pi)$ invariant mass distribution for those candidates with $142 < \Delta M < 149$ MeV. The fitting function is the sum of a Gaussian and an exponential.

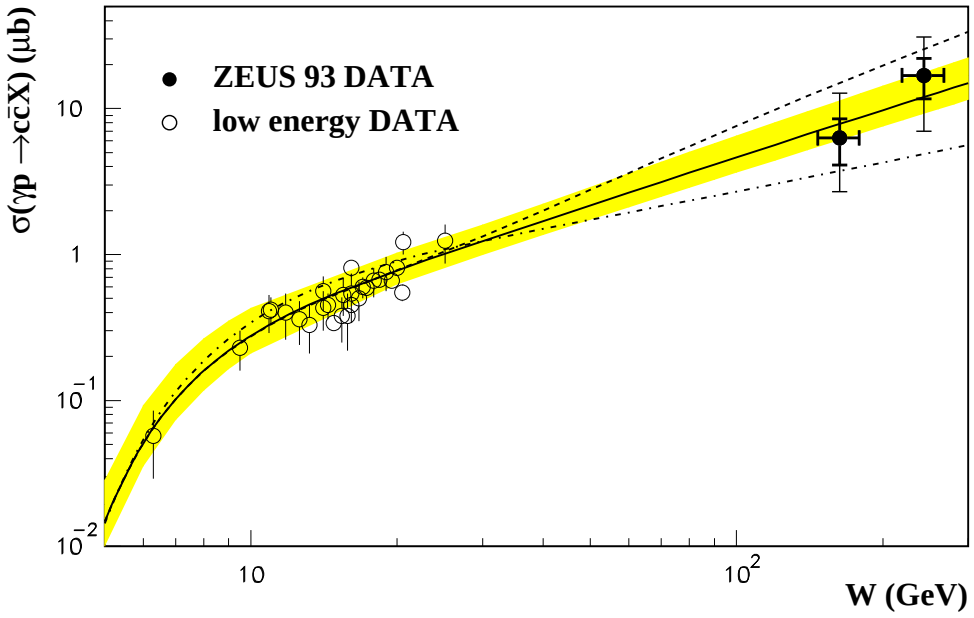

Figure 3: Total $c\bar{c}$ photoproduction cross section as a function of W. The solid dots are the ZEUS measurements and the open dots are earlier measurements from fixed target experiments. The inner error bars are the statistical and the outer ones the systematic errors. The solid line represents the central prediction of NLO calculations with MRSD′_/GRV HO parametrisations of the proton/photon structure function using $\mu_R = m_c$ (for $m_c = 1.5$ GeV) as the renormalisation scale. The shaded band represents the theoretical uncertainties coming from varying this scale in the range $0.5 < \mu_R/m_c < 2$. The dashed line represents the central prediction of MRSD′_/LAC1 and the dash-dotted line is MRSD$'_0$/GRV HO.